# Programmable Diffractive Optical Elements for Extending the Depth of Focus in Ophthalmic Optics

Lenny A. Romero*[a], María S. Millán[b], Zbigniew Jaroszewicz[c], Andrzej Kołodziejczyk[d]
[a]Facultad de Ciencias Basicas, Universidad Tecnológica de Bolivar, Km 1 vía Turbaco, Cartagena, Colombia; [b]Dep. Optics and Optometry, Universitat Politècnica de Catalunya BARCELONATECH, C/ Violinista Vellsolà, 37, 08222 Terrassa (Barcelona), Spain; [c]Institute of Applied Optics, Kamionkowska 18, 03-805 Warsaw, Poland; National Institute of Telecommunications, Szachowa 1, 04-894 Warsaw, Poland; [d]Faculty of Physics, Warsaw University of Technology, Koszykowa 75, 00-662 Warsaw, Poland.

## ABSTRACT

The depth of focus (DOF) defines the axial range of high lateral resolution in the image space for object position. Optical devices with a traditional lens system typically have a limited DOF. However, there are applications such as in ophthalmology, which require a large DOF in comparison to a traditional optical system, this is commonly known as extended DOF (EDOF). In this paper we explore Programmable Diffractive Optical Elements (PDOEs), with EDOF, as an alternative solution to visual impairments, especially presbyopia. These DOEs were written onto a reflective liquid cystal on silicon (LCoS) spatial light modulator (SLM). Several designs of the elements are analyzed: the Forward Logarithmic Axicon (FLAX), the Axilens (AXL), the Light sword Optical Element (LSOE), the Peacock Eye Optical Element (PE) and Double Peacock Eye Optical Element (DPE). These elements focus an incident plane wave into a segment of the optical axis. The performances of the PDOEs are compared with those of multifocal lenses. In all cases, we obtained the point spread function and the image of an extended object. The results are presented and discussed.

**Keywords** extended depth of focus, diffractive optical elements; ophthalmic optics, visual optics, spatial light modulator.

## INTRODUCTION

In any optical imaging system, defocus is the most common and important source of image degradation, which affects the maximum achievable lateral resolution. The DOF is defined as the range along the axis in the object space where images with high lateral resolution can be formed. Conversely, the DOF is the axial range in the image space where images of high lateral resolution are formed for a fixed object position. Outside this range, defocus causes a spatial low-pass filter effect that can be described mathematically in terms of the pupil function and the optical transfer function of the system. There have been several research efforts aimed at resolving this disadvantage. A large number of refractive as well as diffractive optical elements (DOEs) have been designed to overcome this situation and obtain an extended depth of focus (EDOF). In fact, there are many different approaches for achieving EDOF. However, the most promising optical elements for imaging with EDOF in real-time seem to be optical elements focusing an incident plane wave into a focal line segment. These elements can be regarded as modified lenses with controlled aberrations. The modification should lead to output images characterized by the possible highest contrast, brightness and sharpness. Among the most important of these elements we present the Axicon [1], the Axilens [2], the Light Sword Optical Element [3], and the peacock eye [4], [5]. Moreover, there are works that have shown the advantages of these optical elements as an alternative solution to the compensation of ophthalmic aberrations in aged human vision [5]. In this paper we evaluate an optical performance of a variety of programmable DOEs with extended DOF such as: the FLAX, the AXL, the LSOE, the PE, and the DPE. These elements illustrate a potential applicability as EDOF imaging components for presbyopia compensation. The PDOEs will be displayed on a parallel-aligned liquid crystal on silicon spatial light modulator (LCoS SLM), which works in phase only modulation regime [6]. The results obtained with all PDOEs will be compared with a

*lromero@utbvirtual.edu.co; phone 0057 7 6535200 ext 673

10th International Symposium on Medical Information Processing and Analysis,
edited by Eduardo Romero, Natasha Lepore, Proc. of SPIE Vol. 9287, 92871E
© 2015 SPIE · CCC code: 1605-7422/15/$18 · doi: 10.1117/12.2073866



Downloaded From: http://proceedings.spiedigitallibrary.org/ on 05/08/2015 Terms of Use: http://spiedl.org/terms

multifocal lens. The latter consists of three phase diffractive lenses with the same axis that are spatially multiplexed. It has three focal points coinciding with the extremes and the center of the required depth of focus segment [7]. To test the optical performance of all the elements, we obtain the point-spread function (PSF), the modulation transfer function (MTF), and their evolution along the optical axis. To better visualize the imaging performance of each DOE we acquire images of an extended object with incoherent illumination. The MTF is to be computed using a slanted border extracted from the image of the extended object. Additional results concerning incoherent imaging of extended objects placed at different distances are included. The results have been obtained experimentally.

## OPTICAL EXPERIMENT AND PROGRAMMABLE DOES DESIGN CONDITIONS

All programmable DOEs were designed so that the DOF lies within a specific range of focals giving rise to a focal segment within the interval $[f_1, f_2]$ with fixed extremes at the axial distances of $f_1$=30cm (power in diopters of 3.33D) and $f_2$=80cm (1.25D). The Holoeye-HEO LCoS SLM used to display the phase diffractive elements in the experiment has been characterized for an optimized performance as reported [6]. Taking into account the Nyquist criterium for the representation of phase, the pixel pitch (p = 8 microns) of the SLM, the resolution of the device (1920[H] x 1080[V] pixels, of which a square window of size N = 1080 pixels was used to display the computer generated phase DOEs), and the wavelength of the light from a He-Ne laser ($\lambda$=633nm), the shortest focal length was determined by the expression $f_{min}=Np^2/\lambda$ [7]. In our experimental conditions $f_{min}\approx$11cm, thus we have chosen a higher value for $f_1$=30cm. In the case of the single PE had a focal segment $[f_1, f_2]$ that coincided with the requested focal segment, that is $f_1$=30cm and $f_2$=80cm. The double PE had two focal segments $[f_1, f_2]$, and $[f_3, f_4]$, that covered the requested total focal segment, with some overlap (of about 5cm) in the center, that is, $f_1$=30cm, $f_2$=58cm, $f_3$=53cm and $f_4$=80cm. In the optical experiment (Figure 1), each phase diffractive element was displayed on the SLM controlled by computer. A He-Ne laser beam (element 1 in Fig. (1)) was used for illumination. Using a small pinhole (element 4) in the optical axis, the beam was spatially filtered and afterwards collimated to obtain the PSFs produced by each optical element displayed on the SLM (element 9) in the first series of experiments. In the second series of experiments, a ground glass rotating diffuser (element 5) was located against the object (element 6) to obtain incoherent illumination. The extended object was placed at the front focal distance of an auxiliary lens of $f_{aux}$=200mm, thus the image is located at infinity. The extended object used is the figure #2 from the test USAF (1.5mm lateral size) and it covered an angular field ≈0.07'≈4.2". The object was imaged by the DOE displayed on the SLM. A CCD sensor (element 11) was displaced through several planes of the focal segment for capturing the image. We fixed the capturing parameters of the CCD camera (PCO 1600, with large dynamic range of 16 bits) so as to avoid the saturation of the camera.

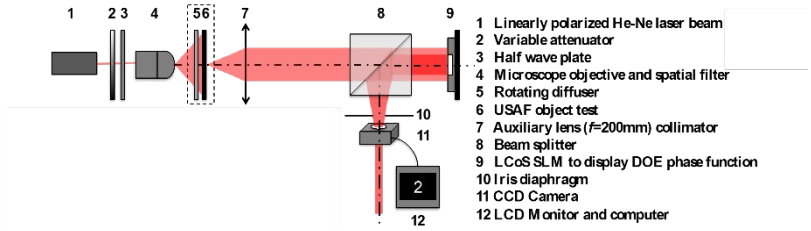


Figure 1. Experimental setup to evaluate the extended depth of focus of programmable DOEs. This setup is used to image a diffusing extended object (element 6) in the second series of experiments. To obtaind the PSFs (first series of experiments) the element 5 and 6 are removed and the element 4 is shift to their position.

## OPTICAL DIFFRACTIVE ELMENTS WITH EXTEDED FOCAL LENGTH

### Forward logarithmic axicon optical element (FLAX)

An axicon is an optical element that transforms an incident plane wave into a narrow focal segment with uniform intensity. The first systematic approach to axicon design in coherent light was presented by Sochacki which is based on energy conservation in ray bundles [1]. It is characterized by a refractive power that decreases with the radial distance ($r$) to its center, thus the peripheral rays are focused to an axial point located farther than the focus for the central rays. Intermediate rays focus to intermediate points, and this is how a focal segment along the optical axis is formed. Figure 2(a) shows the geometrical parameters and distribution of rays for an axicon illuminated by a plane wave of wavelength $\lambda$. The transmittance function for this element has the following form:

$$t(r) = [-ik/2aln(1 + ar^2/f_1)\,], \quad (1)$$



Downloaded From: http://proceedings.spiedigitallibrary.org/ on 05/08/2015 Terms of Use: http://spiedl.org/terms

where $k = 2\pi/\lambda$ and $a = (f_1 - f_2)/R^2 = \Delta f/R^2$ and $r = (x^2+y^2)^{1/2}$. Figure 3(a) shows the resulting phase distribution of this DOE represented in grey levels. This is what is ultimately sent to the modulator.

**Axilens optical elements (AXL)**

This element also concentrates the incoming energy in a segment of the optical axis. It has a focal length that varies with the radial coordinate but the associated phase retardation function differs from the conventional quadratic phase. This element is composed of concentric rings of infinitesimal width. For a conventional lens the transmittance function phase given by $t(r) = [-ikr^2/2f]$, $f$ is a constant independent of $r$. In order to achieve an extended depth of focus in [2] the authors proposed to replace the constant $f$ by an $f(r)$, so that the transmittance function for this element has the following form:

$$t(r) = [-ikr^2/2f(r)], \tag{2}$$

where $f(r)$ is a continuous function instead of a constant and is give by

$$t(r) = f + \Delta f(r/R)^b. \tag{3}$$

Here R is the radius of the lens aperture, $f$ and $\Delta f$ represents the focal of the lens and the length of the focal segment respectively. The constant $b$ depends on the desired intensity distribution of the central peak. For a central peak with uniform intensity throughout the focal range $b$ should be equal to 2; for the mathematical derivation the reader is referred to [2]. The geometrical parameters and distribution of rays for the axilens are shown in figure 2(b). In this element the energy that is incident on an annular ring of radius r and width d$r$ is now confined into the section d$z$ on the optical axis z. Figure 3(b) shows the resulting phase distribution of this DOE represented in grey levels which is sent to the modulator. The transmittance function of the axilens is obtained replacing Eq. (3) into Eq. (2), with $b$=2, and can be written as:

$$t(r) = \{-ikr^2/2[f_1 + (\Delta f r^2/R^2)]\}. \tag{4}$$

**Light Sword Optical Element (LSOE)**

This element is a counterpart of the axilens where the radial modulation of the focal has been replaced by an angular one [3]. The transmittance function has the following form in the polar coordinate system:

$$t(r,\theta) = \{-ikr^2/2[f_1 + (\Delta f\theta/2\pi)]\}, \tag{5}$$

where $r$, $\theta$ are the radial and angular coordinates respectively. Analyzing Eq. (5), we can see that the phase function of the LSOE is an unconventional Fresnel lens that has a focal length $f + \Delta f/2\pi$. Therefore, the LSOE focuses an incident plane wave into a focal segment $\Delta f$. When $\theta \epsilon [0, 2\pi)$ then the segment is stretched from a distance $f_1$ to a distance $f_1+\Delta f$ in front of the LSOE plane. This segment is oriented perpendicularly to the sector, like is shown in Fig.2(c). Figure 3(c) shows the resulting phase distribution of this DOE represented in grey levels which is sent to the modulator.

**Peacock eye optical element (PE)**

The PE optical element belongs to a class of computer-generated diffractive elements, which are able to concentrate an incident beam into a line segment of programmable length and arbitrary inclination to the optical axis, as well as unrestricted distribution of the longitudinal intensity [4]. The geometrical parameters and distribution of rays for a peacock eye and illuminated by a plane wave of wavelength λ are shown in figure 2(e). In the particular case of the PE element, the focal segment is aligned with the optical axis. The transmittance function of this DOE by which an incident plane wave is focused onto a focal segment of the optical axis with uniform intensity distribution is given by

$$t(x,y) = \left[\frac{-iky^2}{2(Lx/A+d)} - \frac{A}{L}x + \frac{dA^2}{L^2} ln\left|\frac{L}{A}x + d\right|\right], \tag{6}$$

where A is a square aperture uniformly illuminated by a plane wave of wavelength λ. L is the length of the focal segment of extremes [$f_1$ , $f_2$ ]. The central point of this segment is at a distance $d$ from de PE aperture. Figure 3(e) shows the resulting phase distribution of this DOE represented in grey levels. In [4] the authors proposed the name owing to the resemblance of the shape of the phase distribution to an eye in a peacock's feather. A PE element can be treated as a spherical zone plate with an added aberration term resembling the coma. However, the angle between the lines limiting the aberration pattern is 70.53º, whereas for the third-order coma it is 60º.



Downloaded From: http://proceedings.spiedigitallibrary.org/ on 05/08/2015 Terms of Use: http://spiedl.org/terms

**Double Peacock eye (DPE)**

From the phase function of the single PE (Eq.6), which focuses the incident plane wave onto a segment along the optical axis. The Double peacock eye element is made by spatially multiplexing two single PE elements [5] These single PEs elements were designed so that their corresponding focal segments are arranged in such a way that one focal segment is located after the other along the optical axis, with some partial overlapping. The total length covers the required depth of focus. We have considered a Random distribution configuration for the design of the double multiplexed peacock eye. In this configuration the device aperture is segmented into small windows of 3x3 pixels. The phase of either one or the other peacock eye (only one of them) is displayed on each window according to a mosaic random distribution. Figure 3(f) shows the resulting phase distribution of this DOE represented in grey levels to be sent to the modulator.

## EXPERIMENTAL RESULTS

For each one of DOEs the PSF, MTF, and the image of an extended object were obtained optically. We show a comparison between the results obtained for all programmable DOEs presented (FLAX, AXL, LSOE, PE, DPE). The results are also compared with a trifocal Fresnel lens, this lens consists of three phase diffractive lenses with the same axis (coaxial configuration) that are spatially multiplexed. It has three focal points coinciding with the extremes and the center of the required depth of focus segment. For the sake of comparison, the phase codification of the resulting multifocal lens is the same as to that used for the peacock eye (random distribution, see Ref. [7].

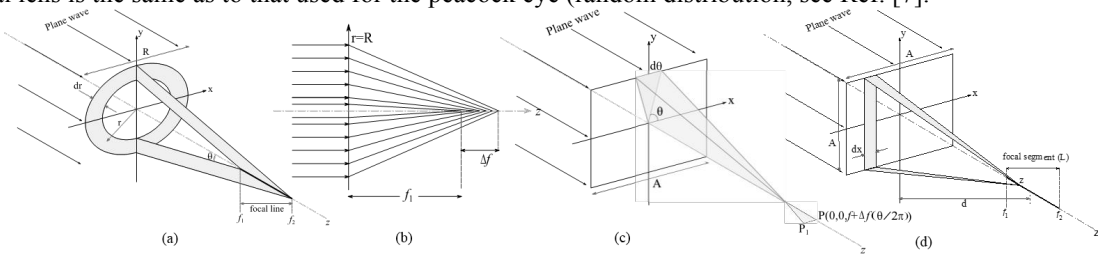


Figure 2. Geometrical parameters and schematic distribution of rays with an input plane wave focused by all DOEs. (a) FLAX, the energy incident on the annulus of radius *r* and width d*r* is equal to the energy on the focal line section of the optical axis, (b) AXL, (c) LSOE, the infinitesimal angular sector of the element focuses an incident plane wave onto a segment PP1 oriented perpendicularly to the optical axis, (d) PE.

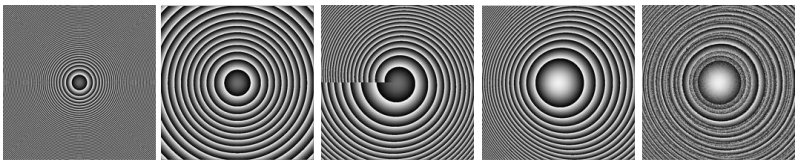


Figure 3. Phase distributions for the PDOEs in represented in grey levels. (a) FLAX, (b) AXL, (c) LSOE, (d) PE,(e) DPE.

Figure 4 shows the experimental results for the PSFs and the images of the extended object along different positions of the focal segment obtained for the different DOEs. Figure 5 shows experimental MTFs calculated from the PSF of the DOEs (Fig 4). The spatial frequency of the MTFs is normalized for the all cases. As for the constant of normalization, we have considered the diffraction-limited cutoff spatial frequency in the object space, in our experiment $f_{\text{cutoff}}$ =238 cycles/degree. For the some DOEs, we present two cross-sections of the MTFs corresponding to perpendicular directions, horizontal (H) and vertical (V).

An overview of the image quality produced by all DOEs along the focal segment reveals that with the exception of the multifocal lens, all remaining elements extend the DOF. However, not all elements preserve image quality significantly along the focal segment. In both the Axicon and Axilens, their PSFs collect most of the incident energy in the central maximum. However, the energy collected around external rings is not negligible, which leads to a decrease in image quality. Because the central maximum concentrates most of the energy along several planes of the focal segment, the DOF is extended. In the case of the FLAX it performs sufficiently well in the first half of the focus range and the performance decreases for the following planes, although it is not a considerable decline. The best image quality appears in the planes of the focal segment, roughly from 30cm to 50cm. In the case of the AXL the best image quality appears in



Downloaded From: http://proceedings.spiedigitallibrary.org/ on 05/08/2015 Terms of Use: http://spiedl.org/terms

the planes of the focal segment from 40cm to 80cm. Analyzing the MTF of the axicon we can see that for distances greater than z = 50cm the MTFs decrease rapidly from the zeroth frequency onward. There are contrast inversions that produce blurry images. In contrast to the effect observed in the MTFs of the axicon, the MTFs of the axilens do not decrease as rapidly and have greater resemblance between them. Which means that it is more insensitive to misfocus than the axicon. This is evidenced by the images of the extended object, which is better defined throughout most of the focal range Δz.

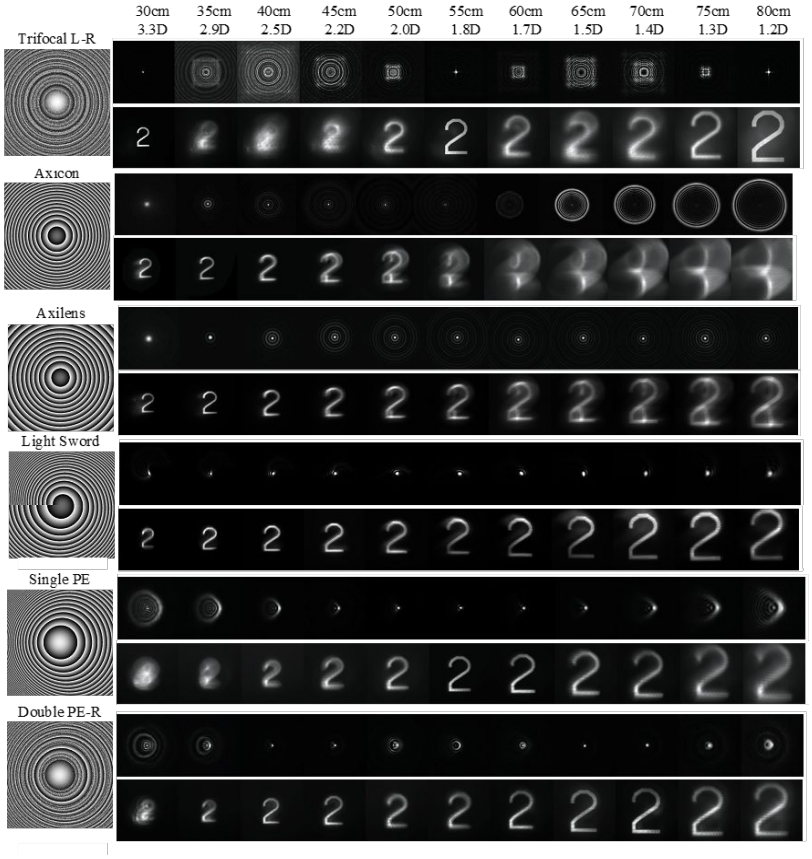


Figure 4. Experimental PSFs and images of an extended object along different positions of the focal segment obtained with the phase of the PDOEs represented in gray levels on the left column. The positions from the DOE (top) are expressed in cm and diopters (D).

The LSOE collect a high amount of incident light at the most intense part of the maximum. These elements have the property of focusing within a focal segment, however the main maximum is not located on the optical axis. From the experimental results, we have located and plotted a series of maxima along the focal segment for different image planes for both elements. In the case of the LSOE it performs sufficiently well in the intermediate image planes and the performance decreases at the extremes ($f_1$=30cm and $f_2$=80cm), although it is not a considerable decline. The best image quality appears in the planes near the central part of the focal segment, roughly from 50cm to 70cm. In the focal planes outside this range, the images degrade relatively quickly. These results are consistent with the MTFs shown in Figure 5.

The performances of the peacock-based elements show a real focal segment, somewhat shorter than expected, where defocus is remarkably reduced. In the case of the single peacock eye, the best image quality appears in the central part of the focal segment, let us say, from 50cm up to 60cm. Images degrade rather quickly outside this central part toward the extremes of the designed focal segment (from 30cm to 80cm). In case of the double peacock eyes, however, the image quality benefits from two separate segments of good performance (the first, from 35cm up to 45cm and the second, from 65cm to 75cm), yet maintaining an acceptable performance in the central part (from 50cm up to 60cm) of the total focal segment, where both focal components overlap. Even in the extremes of the total focal. These results shed some light on the problem of designing optical systems with defocus invariance. Moreover, there exists a potential applicability for ophthalmic applications, like in presbyopia compensation.



Downloaded From: http://proceedings.spiedigitallibrary.org/ on 05/08/2015 Terms of Use: http://spiedl.org/terms

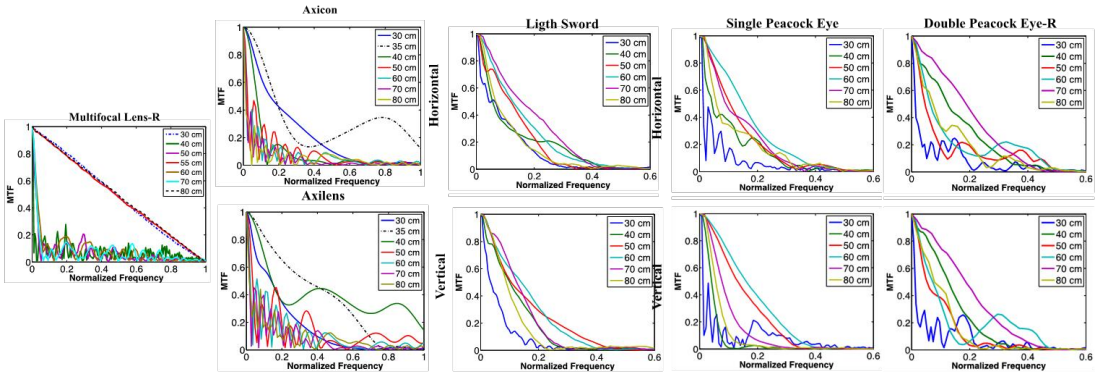


Figure 5. Experimental MTFs computed from the PSFs of Figure 4

## CONCLUSIONS

The experimental results presented in this paper prove that the programmable DOE, designed to focus an incident plane wave into a segment of the optical axis, satisfactorily performs as an EDOF imaging component. We have implemented several programmable DOEs with extended depth of focus such as: the Forward Logarithmic Axicon (FLAX), the Axilens (AXL), the Asymmetric Phase Mask (APM) combined with a mono-focal Fresnel lens, the Light Sword optical element (LSOE), the Peacock Eye (PE), and the double Peacock Eye (DPE) whose phase function is equivalent to the so-called progressive ophthalmic lens. Each DOE has a focal segment that extends between the design focals $[f_1, f_2]$ and its performance has been compared to a programmable trifocal Fresnel lens. We have evaluated the quality of the image formed by each DOE by means of the PSF and the MTF.

The image quality produced by all DOEs along the focal segment reveals that, with the exception of the trifocal lens, all elements are capable of extending the depth of focus. However, not all elements preserve the image quality in a significant way along the focal segment. The FLAX and AXL are the elements that perform worst with the image quality rapidly decreasing from the central part of the focal segment to the extreme of less optical power. Out of all the remaining DOEs, the LSOE and the DPEs are the ones that produce the best image quality along the focal segment. Nonetheless, these elements also display a loss of resolution and contrast. Therefore, the results suggest that a trade-off between the extended depth of focus and image sharpness should be achieved depending on the application. Moreover, these results open new avenues for the design of optical systems invariant to defocus oriented toward ophthalmic applications, like the compensation of presbyopia.

## ACKNOWLEDGEMENTS

This study was partially supported by project DPI2013-43220-R from the Spanish Ministerio de Economía y Competitividad and FEDER.

## REFERENCES

[1] Davidson, N., Friesem, A. A., & Hasman, E. (1991). Holographic axilens: high resolution and long focal depth. Optics letters,*16*(7), 523-525.
[2] Sochacki, J., Bara, S., Jaroszewicz, Z., & Kolodziejczyk, A. (1992). Phase retardation of the uniform-intensity axilens. Optics letters, 17(1), 7–9.
[3] Kolodziejczyk, A., Bará, S., Jaroszewicz, Z., & Sypek, M. (1990). The light sword optical element—a new diffraction structure with extended depth of focus. Journal of Modern Optics, 37(8), 1283–1286.
[4] Jaroszewicz, Z., Kolodziejczyk, A., Mouriz, D., & Sochacki, J. (1993). Generalized zone plates focusing light into arbitrary line segments. Journal of Modern Optics, 40(4), 601–612.
[5] Romero, L. A., Millán, M. S., Jaroszewicz, Z., & Kolodziejczyk, A. (2012). Double peacock eye optical element for extended focal depth imaging with ophthalmic applications. Journal of biomedical optics, 17(4), 046013–1– 046013–8.
[6] Otón, J., Ambs, P., Millán, M. S., & Pérez-Cabré, E. (2007). Multipoint phase calibration for improved compensation of inherent wavefront distortion in parallel-aligned liquid crystal on silicon displays. Applied optics, 46(23), 5667–5679.
[7] Romero, L., Millán, M., & Pérez-Cabré, E. (2010). Multifocal programmable lens: coaxial and multiaxis combination. Opt. Pura Apl, 43(2), 101–112



Downloaded From: http://proceedings.spiedigitallibrary.org/ on 05/08/2015 Terms of Use: http://spiedl.org/terms